Chapter 4
Physical, Nanostructural, and Biocolloid-Chemical Transformations of Marine Iron-Aluminosilicate Sediments and Their Chemical, and Mineral Ore Conversions

A. V. Panko, I. G. Kovzun, V. A. Prokopenko, O. M. Nikipelova, O. A. Tsyganovich, and V. O. Oliinyk

4.1 Introduction

Natural disperse rocks in form of polymineral nano- and microdisperse iron-aluminosilicate systems and materials (IASs) are common in the earth's crust. Colloid-chemical research of transformations of such systems and materials based on iron and iron-manganese ores, marine and lake sediments (oozes), and sands of different origins attracts great attention in recent decades [1–7]. They have been actively studied not only from the viewpoint of the influence on their properties of physical processes but also of colloid-chemical, nanochemical, and physicochemical geomechanics laws [3–7] to find out the mechanisms of complex biocolloidal interactions [3, 8, 9]. However, the interpretation of such influences on polymineral IASs in many specific cases is not yet completed because of the uncertainty of complex physical, physicochemical, geomechanochemical, colloid-chemical, biocolloidal, and

---

A. V. Panko (✉) · I. G. Kovzun · V. A. Prokopenko · O. A. Tsyganovich · V. O. Oliinyk
F.D. Ovcharenko Institute of Biocolloidal Chemistry of NAS of Ukraine, 42, Ak.Vernadskogo Blvd, Kyiv 03142, Ukraine
e-mail: phd.wiz@gmail.com

V. A. Prokopenko · O. A. Tsyganovich
National Technical University of Ukraine «KPI», 37, Peremohy Ave., Building 4, Kyiv 03056, Ukraine

O. M. Nikipelova
Engineering and Technology Institute "Biotechnika" of NAAS of Ukraine, Maiakska St, 26, Khlibodarske, Odes'ka Oblast 67667, Ukraine

Odessa State Environmental University, Lvivska Str., 15, Odessa 65016, Ukraine

O. Fesenko and L. Yatsenko (eds.), *Nanooptics and Photonics, Nanochemistry and Nanobiotechnology, and Their Applications*, Springer Proceedings in Physics 280, https://doi.org/10.1007/978-3-031-18104-7_4

biomedical methods of their research and the ambiguity of relevant conclusions. In general, it is known that physical, physicochemical, colloid-chemical, nanochemical transformations, and contact interphase interactions in marine IASs based on clay-containing sediments aided with bacterial processes lead to the chemical–mineralogical transformations and formation of new disperse polymineral materials with new properties, which may deteriorate under the action of anthropogenic polluting surfactants. Such IASs consist of iron, aluminum, and silicon oxides, and also, but in smaller quantities, of many other inorganic and polluting organic components. The role of the last ones in similar processes is not clear yet [8–25].

The practical importance of both IASs and nanostructural materials extracted from them is growing permanently. That is why the attention to them of technologists and researchers studying not yet established fundamental transformation mechanisms of IASs and relevant materials is growing as well. Thus, synergic, nanochemical, mechanochemical, nanostructural, and other transformations of IASs' components have been studied not enough [1–3]. These transformations in inorganic systems and compositions with bio-originated materials have not yet found their generalized solution.

Thus, the mentioned considerations show the significant actuality of the questions and the necessity of their solution by conducting relevant systematic experimental, model, and theoretical research of disperse iron-aluminosilicate systems and materials for further generalization of the mechanisms of their transformation into new compositions and ore materials.

4.2 Materials and Methods

Preliminary investigations showed that as a result of the influence on microdisperse and nanodisperse IASs, various interactions between their components are possible [3–6, 12, 13]. Such interactions give new properties and change characteristics of IASs. Concerning the said above, the choice of study materials was based on samples with typical colloid-chemical properties usual for most IASs. Earlier [1–6] there were chosen some examples of iron-aluminosilicate materials: different soils and clays; polymineral iron-aluminosilicate compositions extracted from iron ores; pelagic shallow-water and deep-water sediments of the Black Sea and the Azov Sea as model objects for studying the oceanic basins. The chemical composition of general materials used in the study is given in Table 4.1. Materials and compositions were purified by standard methods [7] and powdered up to particle sizes of 63 μm. XRD and X-ray fluorescence investigations of polymineral disperse systems and compositions [1, 13] showed that their structure includes minerals of kaolinite, illite, montmorillonite, glauconite, saponite, goethite, and others. The composition of fine fractions has a lower content of mixed layer formations of montmorillonite-illite and glauconite types.

Table 4.1 Chemical composition of iron-aluminosilicate materials

Oxide content wt%	Polymineral iron-aluminosilicate compositions			Saponite-goethite composition	The Black Sea ooze	River sand	Montmorillonite
SiO_2	18.34	18.31	19.46	46.73	54.57	98.83	49.52
Al_2O_3	2.09	1.76	1.93	5.12	11.35	0.06	21.06
Fe_2O_3	3.18	8.34	2.79	2.76	5.54	1.05	2.72
FeO	56.15	49.23	51.16	23.21	–	–	–
CaO	2.17	1.65	1.98	3.87	8.87	0.01	5.7
MgO	0.73	0.61	0.56	11.43	1.80	–	1.61
MnO	2.48	3.24	7.87	0.35	0.04	–	–
Na_2O	0.45	0.31	0.24	0.82	1.19	–	0.37
K_2O	0.33	0.25	0.26	0.36	1.86	–	0.28
LOI	14.21	16.26	13.67	8.57	13.03	–	17.98

LOI—loss of ignition

Investigations of IASs included using theoretical modeling methods and experimental methods: chemical, rheological, XRD, thermogravimetric, SEM, and biomedical methods [3, 4, 6, 8, 9, 13]. Chemical and X-ray fluorescence analysis used in sample tests was done by the known methodology of qualitative and quantitative methods of analysis of iron-aluminosilicate rocks. X-ray diffraction (XRD) sample analysis was done using diffractometer Dron-UM-1 with CoK_α emission and nickel filter at room temperature. The diffractometer was connected to a computer for diffraction pattern recording. The recording was conducted at 1 degree per minute speed. Registration of X-ray emission was done by scintillation counter BDS-6. Electron microscopy of tested samples: Electron microscopic images were received on electron microscope Selmi PEMU in light field mode. There were also used scanning electron microscopes TESLA BN, JEOL NeoScope JCM-5000, and JEOL JSM6490 LV with INCA ENERGY-450 (Oxford) energy-dispersion device. Thermogravimetric analysis (TGA) was done on thermogravimetric analyzer MOM Q-1500 D (Hungary). Rheological characteristics of investigated systems and materials were determined also by a rotational viscometer with coaxial cylinders Rheotest-2 connected to a computer.

4.3 Results and Discussion

4.3.1 Current Status of Iron-Aluminosilicate System (IASs) Studies

Studying the laws of complex processes in IASs and IASs is the primary source of information about mechanisms of transformation of such systems and materials in natural and technogenic conditions. Substantiated ideas concerning this subject also allow the prediction of the behavior of natural rocks [1, 3–15] as the main compounds of relevant systems and materials in natural, technological, biomedical, and other processes. Thus, such researches of IASs are actual for further development of fundamental ideas concerning their natural transformations under the action of external factors and for the creation of modern technological processes.

Widespread in the earth's crust iron-aluminosilicate materials and marine and lake disperse and ultradisperse systems on their basis take an important place among natural dense nanostructural but at the same time porous on nano- and microlevel rocks and technogenic products of their technological processing. Their physicochemical, physicomechanical, and chemical transformations in the earth's crust and reservoirs, generally in seas and lakes, lead to the formation of disperse nano- and microstructured sedimentary materials of polymineral composition [15]. Their main components are oxides of iron, silicon, and aluminum also containing in iron-aluminosilicates of peloids (Fig. 4.1), but there are many other important compounds contained in clays and oozes as well (Table 4.2). Magnetite and other oxide-hydroxide iron-containing minerals are the most common and present in the most valuable sediments [3, 9–16].

Such sediment minerals have a common effect on the properties of IASs, both in fine-disperse and in dense-fine, and nanocrystalline states. The data in Table 4.3 show that the amount of SiO_2 in sediment samples is the highest and, e.g., reaches 53.93% in red clays, 24.23 and 67.36% in limestone and silica ooze, respectively. A significant amount of Al_2O_3 also shows that the three mentioned oxides (Fe_2O_3, SiO_2, Al_2O_3) play a general role in structural transformations of sediments and MnO_2 (Table 4.1)—in the formation of iron-manganese nodules. Limestone ooze, which contains up to 57% of $CaCO_3$, also has a significant biocolloidal and colloid-chemical effect of calcium minerals [4]. Therefore, the disclosure of the mechanisms of these effects to clarify them requires an additional theoretical, model, and experimental studies.

The distribution of different sediments is presented in Table 4.3. Sizes of nanoparticles in the composition of most distributed red clays are 27.0–86.7 nm [15]. That is why red clays as most important in marine sediments can be attributed to nanostructural materials. However, the nanoparticles' specific role in the deep-sea oozes' composition had almost no research [3, 14, 15]. Shallow-water oozes (diatomic and shelf ones) have a highly disperse microstructure, and the size of ultradisperse particles of about 170–190 nm. Interestingly, the most widespread clays in oceans are red ones containing about 9% of iron oxides (Table 4.2). Their distribution in the World

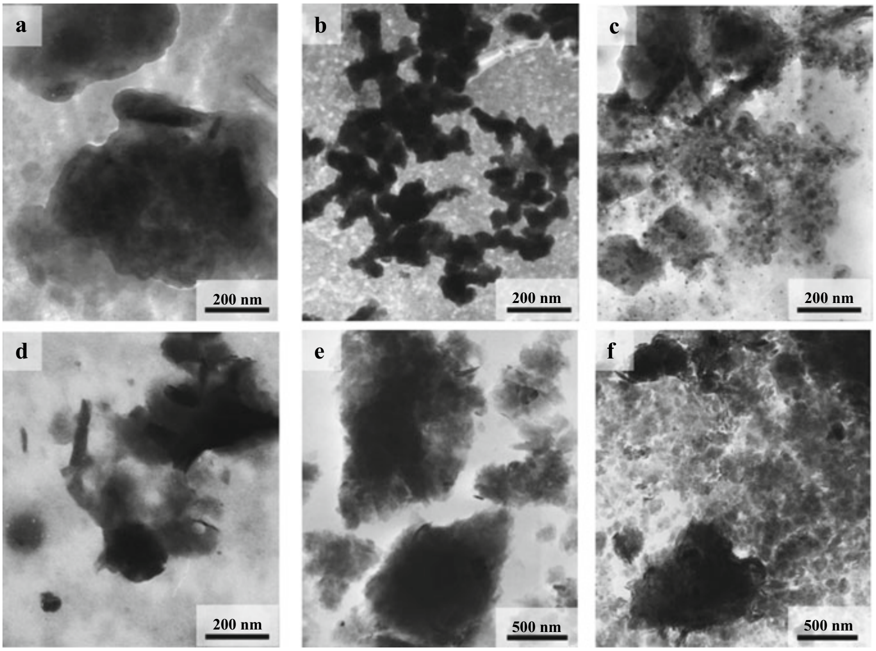

Fig. 4.1 SEM images of peloid sediments and clays: **a** Black Sea sediment. **b** Kuyalnik sediment. **c** Azov-black sea sediment. **d** Bentonitic clay. **e** Glauconite. **f** Hydromica

ocean is the biggest and reaches 540 × 10^6 km^2, including pelitic and terrigenous oozes [3]. Therefore, nanostructural–nanochemical phenomena in IASs, modeling the behavior of red clays without and with the participation of biogeocenoses and their influence on geomechanical, usual, and critical phenomena accompanying mechanodispersive deformations in IASs both on the earth's surface, and in the ocean depths were considered in the first place.

4.3.2 Analysis of Experimental Data Using Theoretical and Model Conceptions

For this analysis, it is important the ideas about the mechanical and nanochemical or (auto-) self-dispersion of IASs in the presence of aqueous mineralized aqueous solutions, as well as natural or anthropogenic surfactants of various origins.

The mechanism of hydrolytic destruction of siloxane bonds of silicate materials [3] is the basis of abiotic mechanical and nanochemical self-dispersion [18] with the aid of water:

Table 4.2 Chemical composition of some usual samples of marine peloid sediments [3, 14–16]

Component	Red clay (%)	Limestone ooze (%)	Silica ooze (%)
SiO_2	53.93	24.23	67.36
TiO_2	0.96	0.25	0.59
Al_2O_3	17.46	6.60	11.33
Fe_2O_3	8.53	2.43	3.40
FeO	0.45	0.64	1.42
MnO	0.78	0.31	0.19
CaO	1.34	0.20	0.89
MgO	4.35	1.07	1.71
Na_2O	1.27	0.75	1.64
K_2O	3.65	1.40	2.15
P_2O_5	0.09	0.10	0.10
H_2O	6.30	3.31	6.33
$CaCO_3$	0.39	56.73	1.52
$MgCO_3$	0.44	1.78	1.21
C_{org}	0.13	0.30	0.26
N_{org}	0.016	0.017	–
Total	100.20	100.17	100.10
Total Fe_2O_3	9.02	3.14	4.98

Table 4.3 Area (in 10^6 km^2) of dissemination of pelitic sediments [3, 14–16]

	Atlantic Ocean		Pacific Ocean		Indian Ocean		Total	
	Surface	%	Surface	%	Surface	%	%	Surface
Limestone oozes	41.6	67.5	51.9	36.2	34.4	54.3	127.9	47.7
Silica oozes	4.1	6.7	21.0	14.7	12.9	20.4	38.0	14.2
Red clay	15.9	25.3	70.3	49.1	16.0	25.3	102.2	38.1
Total	61.6	100.0	143.2	100.0	63.3	100.0	268.1	100.0

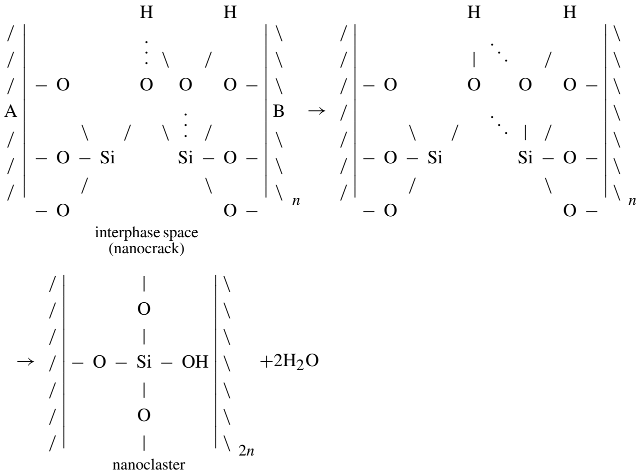

(4.1)

where / / /—surface of micro- and macroparticles; *n*—the number of siloxane groups in the phase contacts in the interphase space.

According to the Gibbs–Smith condition, the intergranular boundaries between the microcrystalline formations *A* and *B* can also be supplemented by the formation *C* (aqueous solution) [18]:

$$\sigma AB > \sigma AC + \sigma BC \tag{4.2}$$

described by the linear-parabolic equation:

$$\mathrm{AL} + \mathrm{BL}^2 = t, \tag{4.3}$$

where *t* is the time of penetration of the liquid at a distance *L*.

The linear part of (4.3) is determined by the kinetics of crystallization pressure increasing P_{cr}:

$$A = \delta \mathrm{RT}/D_{\mathrm{SL}} C_0 P_{\mathrm{cr}} \omega, \tag{4.4}$$

where δ is the average grain size.

The application of the Poiseuille equation gives the following expression for the value of *B* in (4.4):

$$B = 12\eta/\delta P_{\mathrm{KP}} \tag{4.5}$$

where η is the viscosity of the fluid.

Evaluation of 1/*B*, as a conditional dispersion factor, gives values at the level of 10^{-3}–10^{-4} cm^2/s, which is many orders of magnitude higher than the diffusion coefficient in solids. Therefore, the dispersion rate should increase synergistically depending on the grain size (δ). That is, (4.5) confirms the importance of the synergism phenomenon influence [2] on the mechanism of self-dispersion. But the mechanism of this phenomenon has not been previously formulated and has not been associated with synergistic processes in the conditions of simultaneous influence of various factors (mineralized water, surfactants presence) on the behavior of IASs.

In addition to the considered processes of IASs' fracturing, there is also a much more intensive natural and technogenic biotic dispersion of porous materials in various surfactants produced by bacteria in biogeocenoses while the process of metabolism. Analysis of the mechanism of such processes, which are also synergistic and symbate, showed that they are being accelerated by many orders of magnitude [1, 3–6, 8–10, 13, 18]. In this case, their kinetics is described by the equation:

$$(S - S_0)^2 = \mathrm{kt}, \tag{4.6}$$

where S_0 is the initial specific surface of the porous body.

The processes in (4.2)–(4.6) are only physical. At the same time, the substantiation of the water influence on the dispersion of rocks by (4.1) considers the crystallization pressure in nanopores, which can be created only by nanochemical reactions of mineral nanophase formation on a surface in the form of phase contacts. Therefore, more extensive ideas about the mechanism of volumetric pressure in the nanopores of IASs due to nanochemical reactions of polymineral iron-aluminosilicate, aluminosilicate, and silicate nanophases formation are given. They wedge nanocracks in the conditions of synergetic processes (Fig. 4.2a, b) and are formed, for example, according to the reactions:

$$\begin{aligned}&(\mathrm{MnO_2})\mathrm{Fe_2O_3}\cdot \mathrm{nAl_2O_3}\cdot \mathrm{mSiO_2}\cdot \mathrm{kH_2O} + 4\mathrm{MOH} + (\mathrm{k}-1)\cdot \mathrm{H_2O} \rightarrow\\ &\rightarrow \mathrm{M_2O}\cdot \mathrm{nAl_2O_3kH_2O} + \mathrm{M_2O}\cdot \mathrm{mSiO_2}\cdot \mathrm{kH_2O} + \mathrm{Fe_2O_3}\cdot \mathrm{H_2O} + \mathrm{MnO_2}\cdot \mathrm{H_2O}\end{aligned} \tag{4.7}$$

While the reaction products (4.7) react according to the scheme:

$$\begin{aligned}&\mathrm{M_2O}\cdot \mathrm{nAl_2O_3}\cdot \mathrm{kH_2O} + \mathrm{M_2O}\cdot \mathrm{mSiO_2}\cdot \mathrm{kH_2O} \rightarrow\\ &\mathrm{M_2O}\cdot \mathrm{nAl_2O_3}\cdot \mathrm{mSiO_2}\cdot \mathrm{kH_2O} + 2\mathrm{MOH} + (\mathrm{k}-1)\mathrm{H_2O}\end{aligned} \tag{4.8}$$

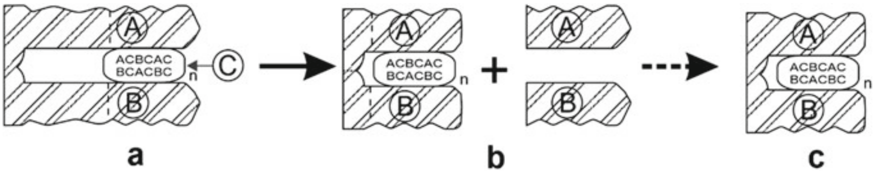

Fig. 4.2 Model of self-hydrational [18] dispersion of rocks with the formation of a new phase: **a** and **b** initial products composed of different minerals, **c** solution of surfactants in water (metabolic products), *n*—nanophase contact capable of dispersion **b** or compaction **c**

Alkaline components and water (4.8) react then according to the scheme (4.7) in cyclic repetitions. That allows almost infinite dispersion with small amounts of alkali and water.

Then, along with $Fe_2O_3{\cdot}H_2O$, they take part in nanostructural–nanochemical contact phenomena, which can be of dispersing or compacting nature—depending on the process conditions [3].

If the products formed by reactions (4.7) and (4.8) have a larger volume than the initial product involved in the reaction (4.7), the resulting pressure breaks (chemically wedges) the crack, which is symbatically facilitated due to the external mechanical load. The water that enters the expanded mouth of the crack hydrolytically breaks up the newly formed secondary nanocracks again by reaction (4.8), and the process of self-dispersion continues with acceleration. The process takes place in the same way as in the case of penetration of liquid phases through intergranular nanoboundaries, but is many orders of magnitude faster and lasts not years, but days or hours. This is also facilitated by other nanochemical interactions in silicate structures, i.e., quartz-like, which complement interactions (4.1), (4.7), and (4.8) and are characterized by the next reactions:

$$(\equiv \mathrm{SiOH})_n + (\mathrm{OH}^-)_n \rightleftarrows (\equiv \mathrm{SiO}^-)_n + n\mathrm{H_2O} \tag{4.9}$$

$$(\equiv \mathrm{SiOH})_n + (\equiv \mathrm{SiO}^-)_n \rightleftarrows (\equiv \mathrm{Si{-}O{-}Si} \equiv)_n \tag{4.10}$$

They also give a start to other nanostructural phenomena of opposite compacting transformations of dispersions due to synergetic coagulation–condensation processes (Fig. 4.2c).

Reactions (4.9) and (4.10) not only complement reaction (4.1) but are also intermediate in the processes (4.7) and (4.8) of the transformation of IASs. The process occurs stepwise, which was shown experimentally on the model system of iron-aluminosilicate–alkaline additive [3].

The generalized chemical models (4.11)–(4.14) of interphase contact interactions of surfaces of disperse iron-aluminosilicate minerals in the composition of iron-aluminosilicate (iron-clay) ore sedimentary materials allow to evaluate the nanocluster biocolloidal mechanisms of such interactions in more details. Thus, with the participation of bacteria, the ferrite formed by reaction (4.7) reacts according to the scheme:

$$\begin{aligned}\mathrm{Fe_2O_3\cdot H_2O_{(micro)}} &\xrightarrow[\text{reduction}]{\text{abiotic}} \mathrm{Fe^{2+}(OH)_2 + Fe^{3+}(OH)_3} \xrightarrow{\mathrm{CO_2}} \mathrm{GR\cdot CO_{3\,(nano)}^{2-}}\\ &\xrightarrow{\mathrm{CO_2+H_2O}} \mathrm{Fe^{2+}(HCO_3)_2(solution)}\\ &\xrightarrow{\mathrm{+O_2}} \alpha-\mathrm{Fe^{3+}OOH(nanogoethite) + CO_2 + H_2O}\end{aligned} \tag{4.11}$$

Then the following biotic phase interactions occur in the contact zones of microparticles:

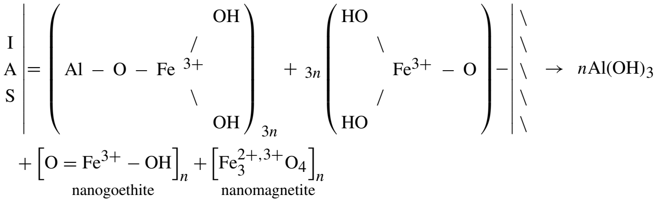

$$\left.\begin{array}{c}\mathrm{I}\\ \mathrm{A}\\ \mathrm{S}\end{array}\right| = \left(\mathrm{Al}-\mathrm{O}-\mathrm{Fe}^{3+}\begin{array}{l}/\,\mathrm{OH}\\ \backslash\,\mathrm{OH}\end{array}\right)_{3n} + 3n\left(\begin{array}{l}\mathrm{HO}\,\backslash\\ \mathrm{HO}\,/\end{array}\mathrm{Fe}^{3+}-\mathrm{O}\right) - \left|\begin{array}{c}\backslash\\ \backslash\\ \backslash\\ \backslash\\ \backslash\end{array}\right. \rightarrow n\mathrm{Al(OH)_3} + \underset{\text{nanogoethite}}{\left[\mathrm{O}=\mathrm{Fe}^{3+}-\mathrm{OH}\right]_n} + \underset{\text{nanomagnetite}}{\left[\mathrm{Fe}_3^{2+,3+}\mathrm{O}_4\right]_n}$$

(4.12)

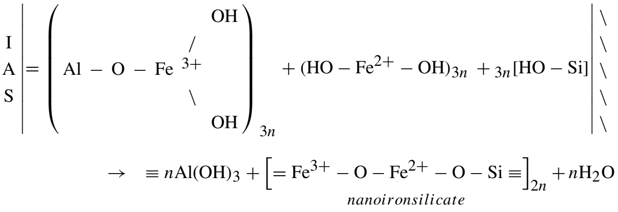

$$\left.\begin{array}{c}\mathrm{I}\\ \mathrm{A}\\ \mathrm{S}\end{array}\right| = \left(\mathrm{Al}-\mathrm{O}-\mathrm{Fe}^{3+}\begin{array}{l}/\,\mathrm{OH}\\ \backslash\,\mathrm{OH}\end{array}\right)_{3n} + (\mathrm{HO}-\mathrm{Fe}^{2+}-\mathrm{OH})_{3n} + {}_{3n}[\mathrm{HO}-\mathrm{Si}]\left|\begin{array}{c}\backslash\\ \backslash\\ \backslash\\ \backslash\\ \backslash\end{array}\right. \rightarrow \ \equiv n\mathrm{Al(OH)_3} + \underset{\textit{nanoironsilicate}}{\left[=\mathrm{Fe}^{3+}-\mathrm{O}-\mathrm{Fe}^{2+}-\mathrm{O}-\mathrm{Si}\equiv\right]_{2n}} + n\mathrm{H_2O}$$

(4.13)

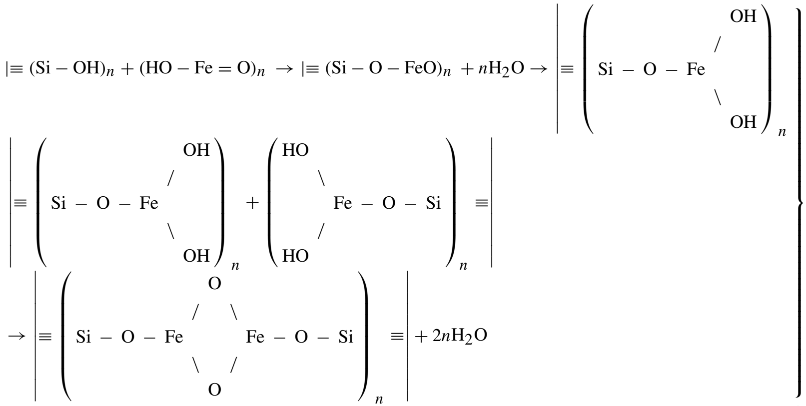

$$\left.\begin{array}{l}|\equiv(\mathrm{Si}-\mathrm{OH})_n + (\mathrm{HO}-\mathrm{Fe}=\mathrm{O})_n \rightarrow |\equiv(\mathrm{Si}-\mathrm{O}-\mathrm{FeO})_n + n\mathrm{H_2O} \rightarrow \left|\equiv\left(\mathrm{Si}-\mathrm{O}-\mathrm{Fe}\begin{array}{l}/\,\mathrm{OH}\\ \backslash\,\mathrm{OH}\end{array}\right)_n\right.\\ \left|\equiv\left(\mathrm{Si}-\mathrm{O}-\mathrm{Fe}\begin{array}{l}/\,\mathrm{OH}\\ \backslash\,\mathrm{OH}\end{array}\right)_n + \left(\begin{array}{l}\mathrm{HO}\,\backslash\\ \mathrm{HO}\,/\end{array}\mathrm{Fe}-\mathrm{O}-\mathrm{Si}\right)_n\equiv\right|\\ \rightarrow\left|\equiv\left(\mathrm{Si}-\mathrm{O}-\mathrm{Fe}\begin{array}{c}\mathrm{O}\\ /\ \ \backslash\\ \\ \backslash\ \ /\\ \mathrm{O}\end{array}\mathrm{Fe}-\mathrm{O}-\mathrm{Si}\right)_n\equiv\right| + 2n\mathrm{H_2O}\end{array}\right\}$$

(4.14)

where (…) n—nanocluster.

As can be seen from models (4.12)–(4.14), the interphase biocolloid interactions (Fig. 4.1) are accompanied by the formation of nanocluster coagulation–condensation bonds between the surfaces of the same or different dispersed phases. That leads to the formation of nanophase contacts (Fig. 4.3) in a structure of iron-aluminosilicate materials. Such mechanisms of contact interactions suggest that Fe^{3+} interactions are stronger than Fe^{2+} interactions because in the latter case, which is characteristic for models (4.11) and (4.13), the microbiological oxidation of Fe^{2+} to Fe^{3+}. Thus, and breaking of interfacial bonds are possible. Thus, the biocolloid mechanism aided with biocenosis differs from the inorganic (abacterial) mechanism without bacterial processes by the intermediate formation of iron-layered double hydroxides (LDH) of Green Rust (GR) type, which include Fe (II) and Fe (III) in their structure.

Studies of biocolloid, bacterial, and biochemical processes based on the use of the phenomenon of selective heterocoagulation of minerals with microorganisms have shown that biogeocenosis, or bio-aggregates formed according to the ideas of

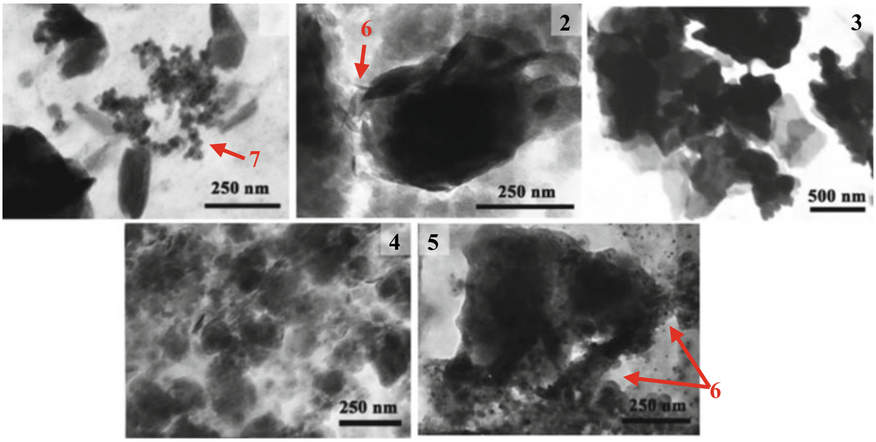

Fig. 4.3 SEM images of montmorillonite (1), hydromica (2), kaolinite (3), glauconite (4), which are the part of typical pelitic sediment (5); zones of phase contacts (6); zone of phase contact formation (7)

biogeochemistry transform into sedimentary deposits and peloids (Tables 4.1, 4.2, 4.3 and 4.4; Figs. 4.1, 4.2, 4.3 and 4.4).

The obtained (Fig. 4.4; Table 4.1) data indicate that bacterial metabolic processes in biocolloidal aggregates lead to the activation of synergetic dispersion of the peloid mineral part according to the mechanisms (4.1), (4.7)–(4.10). Then, upon completion

Table 4.4 Microbiological study of marine peloid samples

Type of microorganism (bacteria)	CFU/cm^3 in peloids		
	Initial	Used	After activation
Cellulose-fermenting • Aerobic • Anaerobic	 10^3 10^1	 10^4 10^1	 10^3 10^1
Butyric acid	10^4	10^2	10^4
Denitrifying	10^2	10^2	10^2
Sulfate-reducing	10^4	10^2	10^4
Nitrifying	10^6	10^5	10^6
Methane-producing	10^7	10^6	10^7
Iron-oxidizing	$3 \cdot 10^6$	$1 \cdot 10^6$	$3 \cdot 10^6$
Ammonificating • Aerobic • Anaerobic	 10^6 10^2	 10^2 10^2	 10^6 10^2
Fat-decomposing	10^2	10^2	10^2
Sulfur-oxidizing	10^4	10^4	10^4
pH	7.4	6.8	7.3

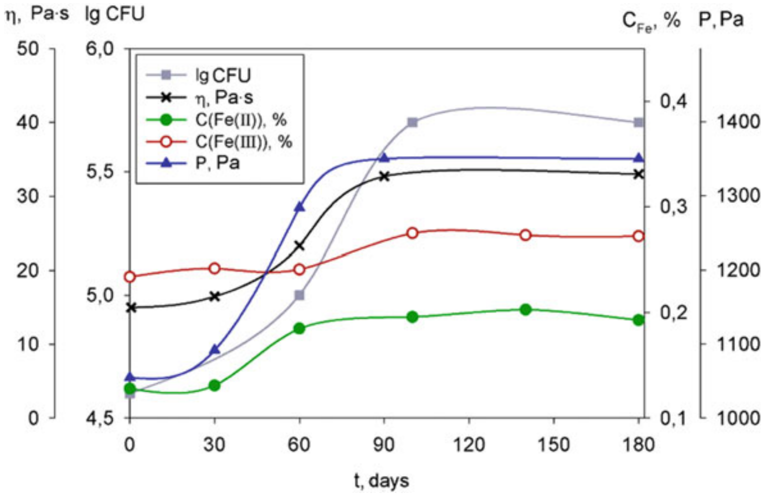

Fig. 4.4 Dependences of viscosity (η), shear stress (*P*), Fe^{2+} and Fe^{3+} concentration (C, %), and the number of colony-forming organisms (lgCFU) in the Black Sea nanostructured iron-aluminosilicate pelagic sediments of 1800 m depth from the time of their exposure; humidity 46%

of the peloid activation process in 90–100 days—to secondary compaction of pelagic sediments due to the repeated increase in the amount of Fe^{3+} in the composition of rapidly decomposing Green Rust according to models (4.11)–(4.14). The optimal ratio of FeO: Fe_2O_3 is close to 1:1 at that. This ratio corresponds to the formation of magnetite, the mechanical properties of which are the highest among iron oxides of various structures. It follows that due to biocolloidal processes, the contact phase nanofilms in the disperse structure are the strongest at an exposure of sediments in the studied interval of 60–180 days (Fig. 4.4)—the formation of magnetite-type nanostructures. This allows scheme (4.11) to be presented for the biocolloidal process as follows [3]:

$$\begin{aligned} Fe_2O_{3(\text{micro})} &\xrightarrow[\text{reduction}]{\text{biotic}} Fe(OH)_2 + Fe(OH)_3 \xrightarrow{CO_2} GR \cdot CO^{2-}_{3(\text{nano})} \\ &\longrightarrow FeO \cdot Fe_2O_3\ (Fe_3O_4)_{(\text{nano})} \end{aligned} \tag{4.15}$$

At that, reactions (4.12)–(4.14) transform on the intermediate stage next way:

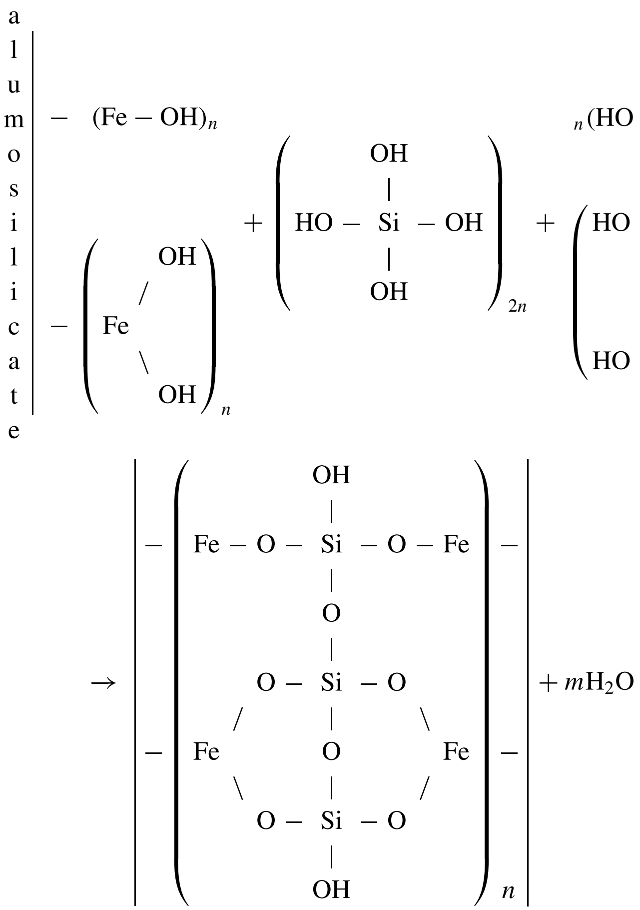

(4.16)

The general model abiotic and biotic scheme of the rock transformation is shown in Fig. 4.5.

According to the data obtained (Tables 4.1, 4.2, 4.3, 4.4 and 4.5; Figs. 4.1, 4.2, 4.3 and 4.4), the greatest influence on the rheological properties of nanostructured IASs has clay minerals, especially montmorillonite, which is a part of bentonite. Therefore, the processes of clay suspension nanostructuring, nanochemical processes of nanoparticle formation in them, including biocolloidal processes, as well as the chemical structure of nanoparticles have a significant impact on the rheological behavior of IAS suspensions. That is shown in Fig. 4.6 for conditions of the viscosity effects of hyper- and ultra-anomaly occurrence.

According to the above curves, hyperanomaly of viscosity is more often characterized by curves 1 and 3, and the previously unknown effect of viscous ultra-anomaly is more usual for curve 2, and sometimes curve 1. Both effects have been experimentally confirmed for numerous rheograms of suspensions for different types of clays, pelitic sediments, and peloids. Therefore, it should be concluded from these data that

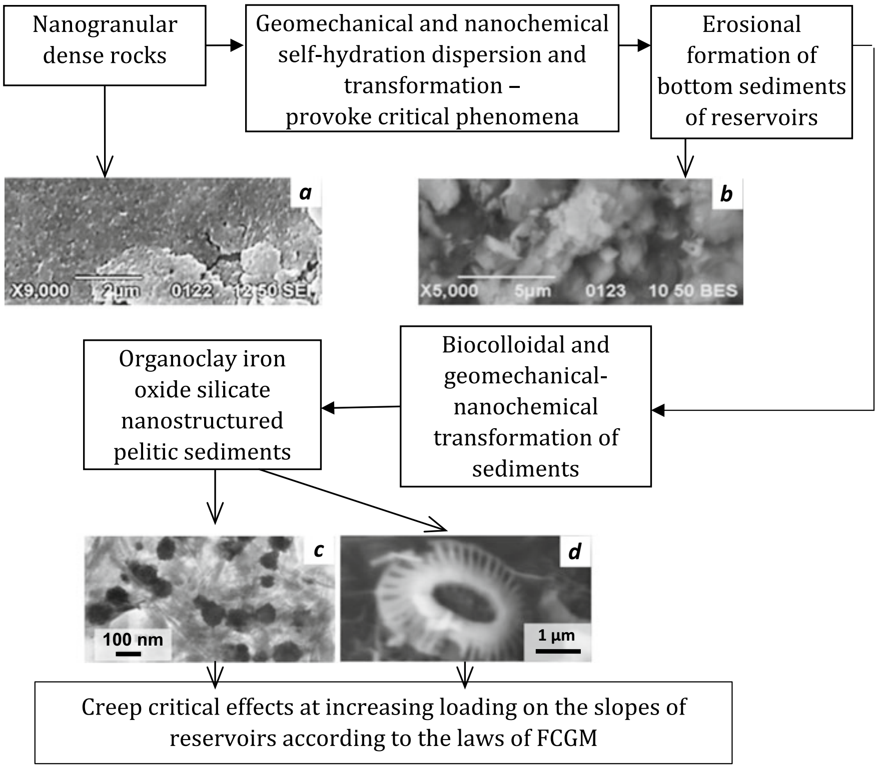

Fig. 4.5 Abiotic and biotic rock transformation general scheme; SEM images of **a** nanogranular rocks; **b** bottom sediments of erosive crushed rocks; **c** pelitic iron-aluminosilicate sediments and peloids; **d** pelitic biotic sediments with carbonate residue of *Foraminifera*

the effect of viscous hyperanomaly is more usual for less concentrated suspensions or with lower iron content in them. On the other hand, the effect of ultra-anomaly of viscosity—for more concentrated suspensions or at lower shear rates with stable other previously mentioned factors. The moisture content of the dispersions (W) changes as follows: $W_{1'-2} < W_{1-2} < W_{1-3}$. If the factors change, i.e., the addition of alkaline additives, the viscosity of iron-aluminosilicate clay sedimentary rock (Figs. 4.4 and 4.7) decreases sharply.

The established regularities allow substantiating the methods of controlling the physicomechanical properties of barrier structures, soils, and rocks with the help of various active environments of natural and technogenic origin.

Thus, theoretical studies and obtained experimental data allowed to consider the thermodynamic basis, kinetics, and mechanisms of transformation of rocks due to their self-hydration spontaneous dispersion [18] aided with nanochemical and bacterial processes with the formation of new disperse structures with thermodynamically stable mineral phases; to develop an idea of the mechanisms of rocks creeping due to

Table 4.5 Physicochemical characteristics of the bottom sediment samples

Index	Saltwater storage pond (Kryvyi Rih)	Kuyalnik Estuary
1. pH of liquid phase	7.7	7.20
2. Redox potential	–	−227
3. Moisture (wt%)	56	58.1
4. Volume weight (g/cm^3)	1.33	1.47
5. Adhesiveness (Pa)	–	833
6. Shear stress limit (Pa)	770	491
7. Concentration of particles $> 250\ \mu$m (%)	1.2	0.61
8. Specific heat capacity (kJ/kg K)	–	0.59
9. Concentration of H_2S (%)	–	0.17
10. Concentration of C_{org} (%)	–	2.06
11. Concentration of particles (1–5 μm) (%)	3.7	2.65
12. Concentration of particles ≤ 100 nm (%)	0.5	0.34

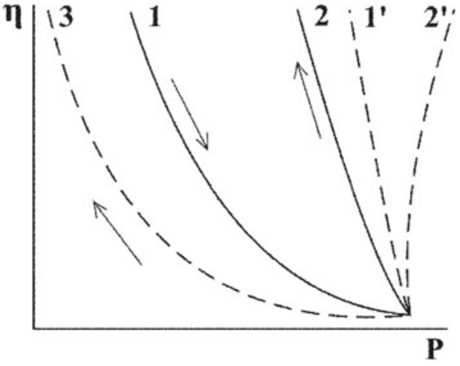

Fig. 4.6 Load and unload curves (1, 1′ and 2, 2′—respectively) in the conditions of plastic flow of elastic–plastic material; 3—unloading curve in conditions of viscosity hyperanomaly beginning [13]

recrystallization of mechanically stressed areas and nanochemical transfer of interfacial boundaries of substances of the liquid phase to other stressed areas of the surface; to reveal the basic global principles of physical–mechanical and nanochemical regulation of structural properties of disperse-porous sediments in natural and technogenic conditions to prevent critical phenomena in them; to outline further ways of developing of these fundamental problems [3].

Analysis of the mechanisms of nanostructured physicochemical transformations of various representatives of IASs and modeling of common and critical creep processes on sea slopes and ocean beds showed that NIASs are generally colloidal oozes and bottom sediments composed of minerals and organic substances that have undergone significant transformations due to geological, geomechanical, chemical, nanochemical, biological, biocolloidal, and other abiotic and biotic processes. They

Fig. 4.7 Influence of the chemical structure of contact silicate nanoclusters on the viscosity of aqueous 50% suspension of iron-aluminosilicate clay pelitic sedimentary rock depending on concentration (*C*) of anionic inorganic nanoclusters of different chemical composition

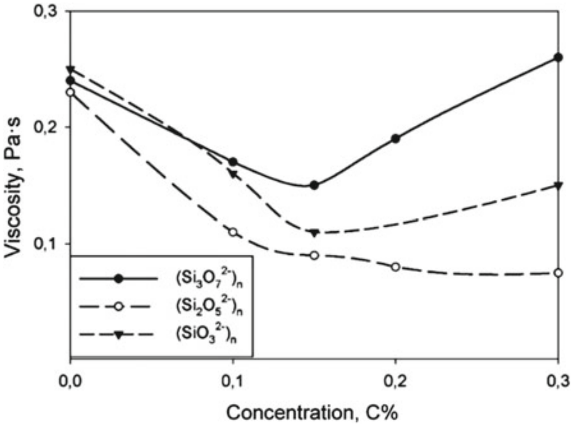

are a homogeneous fine plastic mass. They include natural colloidal, and biocolloidal formations of various origins, such as iron ore formations with a large amount (40–70%) of iron oxides, and admixtures of aluminosilicates and clay minerals with admixtures of iron oxides, as well as freshwater clay soils, sands, and saltwater iron-containing disperse deposits. Sea oozes (Figs. 4.3 and 4.8) or pelitic deposits of coastal and deep-water origin were studied as the main representatives of the NIASs, the share of which reaches 70–80% among the known NIASs. The finding of nanostructural, biocolloidal, physicochemical, and geomechanical mechanisms of their formation was required to answer the system questions of NIASs' participation in usual and critical phenomena, both on the underwater slopes of the seas and oceans, and in the formation processes of ore deposits.

Among the NIASs, the most important from a practical point of view are clays—bounded non-cemented sedimentary rocks of biocolloidal origin with a predominant content of clay minerals with admixtures of iron oxides, sedimentary iron ores, and

Fig. 4.8 Particle size distribution of mud fine-grained fraction: ●●●● mud from the Azov; ▬ mud from the Black Sea, sample 1; --- mud from the Black Sea, sample 2

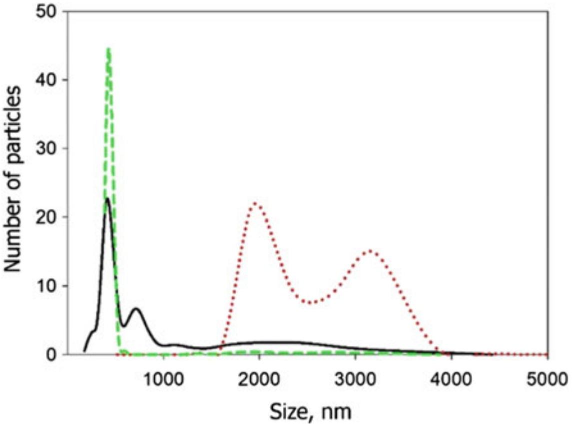

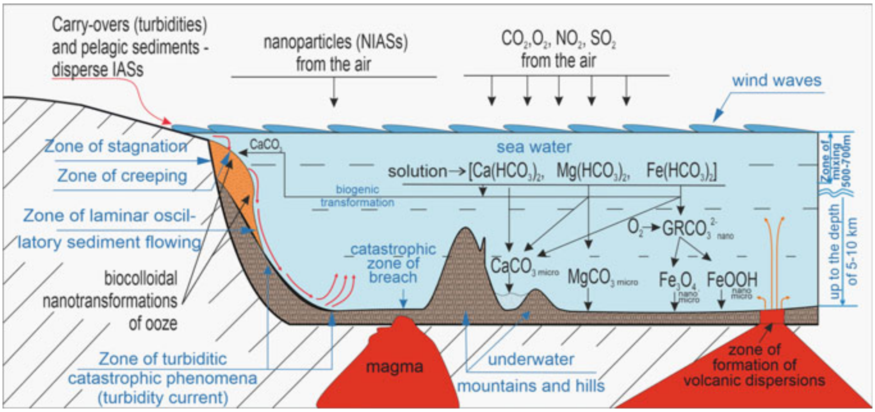

Fig. 4.9 Model of modern nanostructural marine transformations of IASs, pelitic sediments, and turbidites on slopes, gaps, and abyssal plains, accompanied by compacting or ooze flow [1, 3, 14] and stratified sediment separation in processes of ore deposit formation

pelitic deposits (peloids)—sediments of lakes, seas, and oceans. They are composed of planktonic organisms rests, fine-disperse mineral particles, space dust, and products of chemical transformations in fresh and saltwater. Their creep or normal and critical behavior in terms of geomechanical and nanochemical processes is most likely related to the destructive work of water waves of various origins and landslides in water reservoirs. The developed model of these processes for marine sediments is given in Fig. 4.9.

Waves that penetrate to a depth of 600–700 m during storms, and sometimes up to several kilometers (while typhoons or tsunami), create the effect of hydraulic shock, which instantly dilutes thixotropic sediments, turning them into a viscous liquid capable of active nanochemical and geomechanical transformations. The resulting suspension flows down the slope without mixing with water due to the higher specific weight. This, in particular, can explain the appearance of chemically transformed (under the influence of pH changes) clay terrigenous sediments at great depths. In addition, on the slopes of seismic zones of the oceans (Fig. 4.9), which can reach lengths up to 2000 m and more, the speed of mudflows weighing up to hundreds of millions tons of rock increases significantly from laminar (up to 0.5 km/h) to normal fast (up to 40 km/h) and catastrophic (up to 100 km/h) current.

From the process models in Figs. 4.1 and 4.9, and schemes (4.7)–(4.16), it turns out that the interphase biocolloidal interactions are accompanied, with the participation of surface-active products of microorganism metabolism, by the formation of nanocluster coagulation–condensation phase bonds between surfaces of the same or different disperse phases. It leads to the secondary compaction of previously dispersed ferroaluminum silicate materials (Fig. 4.2c). Such mechanisms of contact interactions suggest that Fe^{3+} interfacial interactions are stronger than Fe^{2+}. That is because in the latter case, characteristic for models of surface nanochemical reactions, additional microbiological oxidation of Fe^{2+} to Fe^{3+}, and rupture of interfacial

–O– Fe–O– bonds with the formation of goethite at first, and then magnetite is possible. It coincides with the conclusions of geological science. Thus, the biocolloidal mechanism differs from the previously considered abiotic mechanism by the intermediate formation of Green Rust (GR), which is converted into goethite, magnetite, and siderite or iron-manganese nodules, and other ore minerals. It should be emphasized that the formation of magnetite occurs in anaerobic conditions, but in conditions of the aerobic process, the goethite is formed [3].

It is also possible to provide the scheme for the biocolloidal process in the specified form:

$$\begin{aligned}&\mathrm{Fe_2O_3\cdot H_2O_{(micro)}+H_2O+surfactant}\xrightarrow[\text{reduction}]{\text{microbiological}}\mathrm{Fe(OH)_2}\\&+\mathrm{Fe(OH)_3}\xrightarrow{\mathrm{CO_2}}\mathrm{GR\cdot CO^{2-}_{3(nano)}}\\&\to\mathrm{Fe_3O_{4(magnetite,nano)}}\left[\mathrm{FeOOH_{(gothite,nano)}};\ \mathrm{FeCO_{3(siderite,micro)}}\right]\end{aligned}\tag{4.17}$$

Reactions (4.12)–(4.14) are transforming as follows:

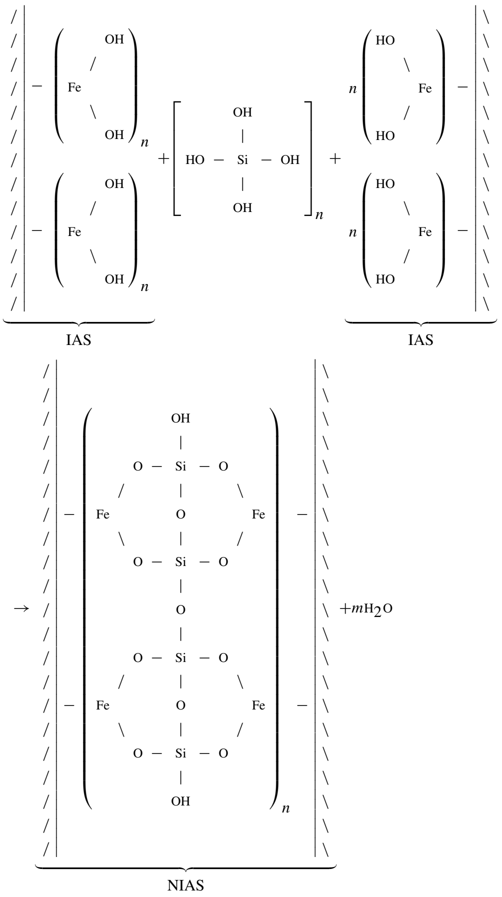

(4.18)

The nanostructuring processes of clay suspensions, nanochemical processes of nanoparticle formation in them, including biocolloidal processes, as well as the chemical structure of nanoparticles have an important influence on the rheological behavior of IASs dispersions, especially in conditions of viscous ultra-anomaly (Figs. 4.10 and 4.11).

Systematic analysis of the study results of nanostructural phenomena in the earth's crust and experimental data on the impact of synergistic nanochemical and microbiological processes on these phenomena indicate a scientifically approved ability to achieve shortly a fairly accurate description of nanochemical and rheological mechanisms of many common and critical sediment movement processes occurring in the earth's crust and on its surface, in reservoirs, seas, oceans, and in technogenic conditions. It also gives an ability to develop the ideas of the mechanisms of mineral deposits biocolloidal formation not only in the Archean but also in the Androgenic era (2.588 million years ago and until today).

Based on the analysis of the obtained results, the colloid-chemical ideas about processes on underwater slopes of seas and oceans in the conditions of the gravitational laminar-turbulent flow of sediments according to the laws of physicochemical geomechanics and laws of elastic–plastic change in viscosity was developed too, taking into account the data provided in [1, 3, 14]. The chemical mechanisms of the main processes in such sediments are as follows:

1. Contact abiotic phase interactions in conditions of viscosity ultra-anomaly effect:

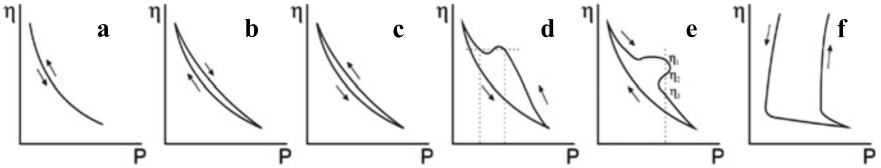

Fig. 4.10 Rheological curves (general view): **a** non-Newtonian fluid; **b** thixotropy; **c** rheopexy; **d** dilatancy; **e** viscous hyperanomaly; **f** ultra-anomaly of viscosity in the transition area to the Atterberg viscosity limit. Wa > Wb > Wc > Wd > We > Wf, where *W* is the water content of the dispersion

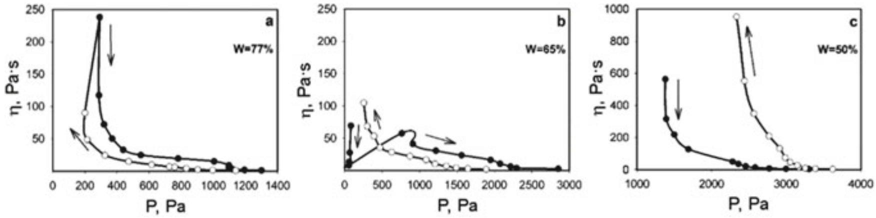

Fig. 4.11 Experimental rheological curves at different humidity (*W*) for the Black Sea pelitic sediment: **a** thixotropy; **b** ultra- and hyperanomaly of viscosity; **c** ultra-anomaly of viscosity

$$\begin{array}{c|}/\\/\end{array} = [\mathrm{Fe-OH}]_n + {}_n[\mathrm{HO-Fe}] = \begin{array}{|c}/\\/\end{array} \longrightarrow \begin{array}{c|}/\\/\end{array} = [\mathrm{Fe-O-Fe}]_n = \begin{array}{|c}/\\/\end{array} + m\mathrm{H_2O}$$

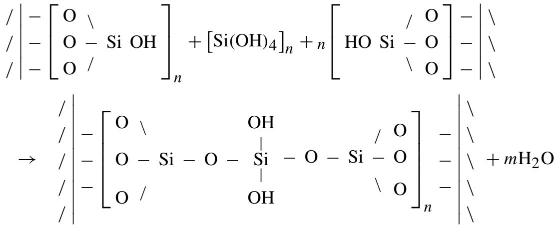

$$\begin{array}{c|c} / & - \\ / & - \\ / & - \end{array}\left[\begin{array}{l} \mathrm{O}\ \backslash \\ \mathrm{O - Si\ OH} \\ \mathrm{O}\ / \end{array}\right]_n + \left[\mathrm{Si(OH)_4}\right]_n + {}_n\left[\begin{array}{r} /\ \mathrm{O} \\ \mathrm{HO\ Si - O} \\ \backslash\ \mathrm{O} \end{array}\right]\begin{array}{c|c} - & \backslash \\ - & \backslash \\ - & \backslash \end{array}$$

$$\rightarrow \begin{array}{c|c} / & \\ / & - \\ / & - \\ / & - \\ / & \end{array}\left[\begin{array}{l} \mathrm{O}\ \backslash \\ \\ \mathrm{O - Si - O - \underset{OH}{\overset{OH}{Si}} - O - Si - O} \\ \\ \mathrm{O}\ / \end{array}\right]_n \begin{array}{c|c} & \backslash \\ - & \backslash \\ - & \backslash \\ - & \backslash \\ & \backslash \end{array} + m\mathrm{H_2O}$$

2. Biocolloid nanostructural–nanochemical process:

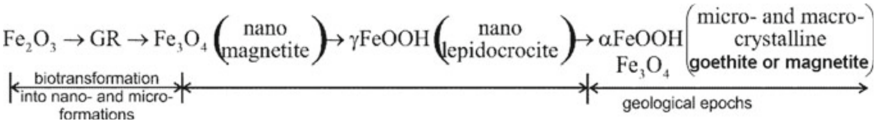

Preliminary data in Table 4.6 and Figs. 4.12 and 4.13 simulate red clays' behavior in mixing conditions during movements on sea slopes. They give an idea of how the dispersion of various IASs goes, including red clays, under the action of surface-active metabolism products of microorganisms from biogeocenoses (Tables 4.4 and 4.5). Such transformations are accompanied by macrostructures' transition into micro- and nanostructured sedimentary formations with their simultaneous separation into layers with different densities and mineralogical composition. They are forming under the influence of the bacterial metabolism of biogeocenoses. Some stages of such complex phenomena are shown in Figs. 4.1, 4.2, 4.3, 4.4, 4.5, 4.6, 4.7, 4.8, 4.9, 4.10 and 4.11. It can be considered expedient to continue such studies to develop marine biocolloidal geoecology ideas by comprehensively studying the mechanisms of deep-water processes of sediment transportation, their layer-by-layer separation, enrichment of formed ore deposits, and further application.

The mechanisms of nanostructural and microstructural biocolloidal transformations, layer-by-layer separation of iron-aluminosilicate turbidite-pelitic sediments were considered too, taking into account the findings of specialists in various scientific fields [1, 3, 14] and experimental data (Figs. 4.12 and 4.13).

Table 4.6 Geomechanical dispersion of aqueous (NaCl = 28 g/dm^3) suspension of iron oxide clayey ore marine sediments under the action of biocolloidal processes

Suspension exposure (days)	Fractions (mm)				
	5–1 mm	1–0.5 mm	0.5–0.05 mm	0.05–0.005 mm	< 0.005 mm
1	21.2	28.7	37.9	8.9	3.3
10	12.3	29.4	40.6	7.9	9.8
15	8.9	25.4	41.3	8.2	13.2
20	7.4	17.7	40.1	14.1	20.7
30	6.8	13.1	37.5	19.3	20.3

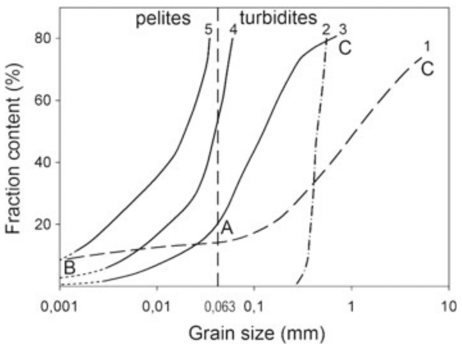

Fig. 4.12 Distribution of grain sizes in the most typical iron-aluminosilicate sediments (based on data from [14]): 1—turbidite-pelitic; 2—sand; 3—clays; 4—loess; 5—siltstone; AB—pelitic fractions (lines 1, 3, 4, 5); AC—turbidite fractions (lines 1, 2, 3, 4)

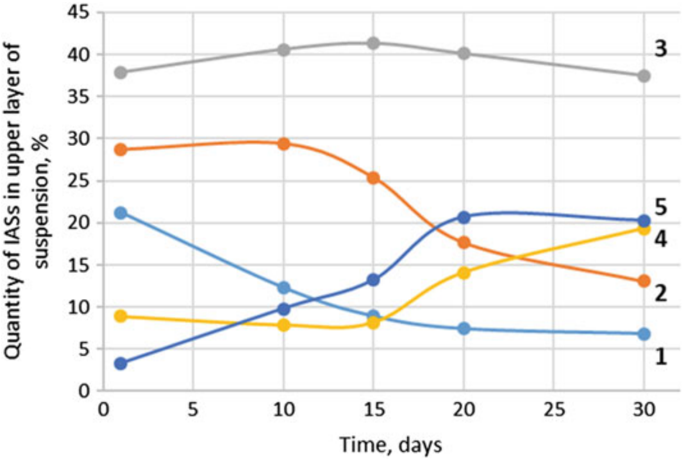

Fig. 4.13 Geomechanical self-dispersion of aqueous suspension (NaCl = 28 g/dm^3) of iron-aluminosilicate marine sedimentary red iron ore of biocolloid origin under the action of biocolloidal processes of its activation. Line number for fractions: 1—5–1 mm; 2—1–0.5 mm; 3—0.5–0.1 mm; 4—0.1–0.05 mm; 5—< 0.05 mm

The mentioned processes significantly depend on the biocolloid transformations of sediments. These transformations combine microstructural and nanostructural geomechanical self-hydrational dispersion of sediments with their simultaneous separation into separate layers under the influence of bacterial metabolism as a part of biogeocenoses. The upper layer of such sediment, which forms in conditions of its rapid mixing or displacement (catastrophic processes of underwater sediments flowing at a speed up to 100 km/h), is enriched in natural conditions under the influence of metabolic products with nanostructured iron hydroxides, calcite, and clay minerals—montmorillonite, hydromica, glauconite, kaolinite. Medico-biological studies have shown that such layers, separated from other sediment layers, have different particle sizes and mineral compositions, as well as different biomedical properties. It is shown that the stratification of suspensions into separate layers occurs during the activation of suspensions with biogeocenoses by nutrient media, i.e., in the conditions of biocolloid and geomechanical processes activation, which last for 5–25 days. Upon completion of these processes, the stratification of suspensions decreases. It was found that the upper layer of suspensions under the brine layer during the activation process hugely enriches with nano- and microparticles of iron and calcium compounds with up to 90–95% purity, and it raises their content in enriched products and increases the therapeutic properties of peloids separated from turbidite-pelagic marine underwater sediments in several times.

It was also established for the first time that the biocolloid treatment of iron-aluminosilicate materials leads to the stratification of suspensions into three layers during the activation process. The middle layer has a higher specific weight than the upper and lower (bottom) layers. The mechanism of such a phenomenon is considered and substantiated.

The results shown in Table 4.7 allow to substantiate the fundamental mechanism of layer-by-layer synergetic [25] separation of ocean red clays with their transition from goethite (tobacco) to red-brown ($2'$, $2''$), and to oolitic ($3'$, $3''$) ores enriched with iron-manganese nodules [15].

4.4 Conclusions

It is shown the interrelation of physical, geomechanical, colloidal, biocolloidal, and other processes in IASs and their complex influence on dispersion, transformation, and subsequent contact interphase nanostructuring, and further chemical transformations of sedimentary deposits of iron-aluminosilicate, and iron oxide-hydroxide materials into ore materials while processes of their self-hydrational separation in several layers.

It is shown and analyzed the generalized physical, nanochemical, mechanochemical, nanostructural, and other transformations of IAS components. It was shown as for separate inorganic iron oxide-hydroxide-silicate systems, first of all, iron oxides and hydroxides, silicate minerals, and quartz and for them in a composition of biocolloidal materials under the action of synergetic phenomena, and processes of symbiosis.

The ideas about complex multifactor mechanisms of IASs transformation are systematized.

An analysis of critical (catastrophic) phenomena and their comparison with usual ones in the earth's crust and on its surface from the viewpoint of colloidal and biocolloidal chemistry is done. That was not done before and is relevant for modern environmental safety.

The effect of ultra-anomalous behavior on marine sediment flow is established. It was explained from the viewpoint of classical mechanics and geomechanics, nanoscience, colloidal and biocolloidal chemistry.

Table 4.7 Results of chemical analysis of biocolloid tobacco (1′, 1″), brown (2′, 2″), and oolitic (3′, 3″) ores of the Azov deposit [15]

Element	Content (%wt)					
	1′	1″	2′	2″	3′	3″
Ag	< 0.01	< 0.01	< 0.01	< 0.01	< 0.01	< 0.01
Al	1.55	1.52	1.46	1.41	1.29	1.29
As	0.12	0.13	0.10	0.11	0.12	0.13
B	< 0.01	< 0.01	< 0.01	< 0.01	0.01	< 0.01
Ba	0.05	0.07	0.14	0.11	0.58	0.62
Be	< 0.01	< 0.01	< 0.01	< 0.01	< 0.01	< 0.01
Bi	< 0.01	< 0.01	< 0.01	< 0.01	< 0.01	< 0.01
Ca	1.62	1.53	1.12	1.18	1.29	1.00
Cd	< 0.01	< 0.01	< 0.01	< 0.01	< 0.01	< 0.01
Co	< 0.01	< 0.01	< 0.01	< 0.01	0.04	0.04
Cr	< 0.01	< 0.01	< 0.01	< 0.01	< 0.01	< 0.01
Cu	< 0.01	< 0.01	< 0.01	< 0.01	< 0.01	< 0.01
Fe	36.11	37.70	30.01	31.82	29.50	29.33
Ga	< 0.01	< 0.01	< 0.01	< 0.01	< 0.01	< 0.01
K	0.23	0.23	0.29	0.27	0.33	0.31
Li	< 0.01	< 0.01	< 0.01	< 0.01	< 0.01	< 0.01
Mg	0.45	0.45	0.29	0.25	0.36	0.23
Mn	0.56	0.70	7.18	6.09	8.81	9.04
Mo	< 0.01	< 0.01	< 0.01	< 0.01	< 0.01	< 0.01
Na	0.07	0.07	0.13	0.12	0.22	0.20
Ni	0.02	0.02	0.11	0.11	0.11	0.12
P	2.01	2.03	0.76	0.79	1.39	0.94
Pb	0.02	0.02	0.01	0.01	0.02	0.02
S	0.04	0.04	0.07	0.09	0.13	0.12
Si	8.31	7.44	7.74	8.07	7.68	8.63
Sn	< 0.01	< 0.01	< 0.01	< 0.01	< 0.01	< 0.01
Sr	0.04	0.04	0.07	0.06	0.11	0.11
Ti	0.12	0.11	0.09	0.08	0.09	0.10
V	0.05	0.05	0.05	0.05	0.05	0.05
W	< 0.01	< 0.01	< 0.01	< 0.01	< 0.01	< 0.01
Zn	0.03	0.03	0.03	0.03	0.03	0.03
Zr	< 0.01	< 0.01	< 0.01	< 0.01	< 0.01	< 0.01

The influence of rheological characteristics of iron-aluminosilicate turbidite-pelitic sediments on the occurrence of their usual and critical flow and the transformation character of the stratified flow is systematized, and the special significance of the phenomena of hyper- and ultra-anomaly is shown.

Research on the interrelated physical, colloid-chemical, biocolloid, nanostructural, and other features of usual and critical transformations of polymineral iron-aluminosilicate estuarine, marine, and oceanic sediments may become a new area of research on their global impact on the flowing of such sediments not only in terms of marine geology but also considering the further pollution of the oceans when the critical phenomena become much greater. On the other hand, colloid-chemical and biocolloid approaches will be able not only to explain more deeply the physical appearances of such flow but also to provide real tools to predict and prevent critical (catastrophic) occurrences with an application of obtained results.

References

1. Gomes C, Carretero M-I, Pozo M, Maraver F et al (2013) Peloids and pelotherapy: historical evolution, classification and glossary. Appl Clay Sci 75–76:28–38
2. Carretero MI (2020) Clays in pelotherapy. A review. Part I: mineralogy, chemistry, physical and physicochemical properties. Appl Clay Sci 189:105526. https://doi.org/10.1016/j.clay.2020.105526
3. Kovzun IG, Prokopenko VA, Panko AV, Tsyganovich OA, Oliinyk VO, Nikipelova OM, Ulberg ZR (2020) Nanochemical, nanostructural and biocolloidal aspects of transformations in dispersions of iron-aluminosilicate minerals. PH “Akademperiodyka”, Kyiv. https://doi.org/10.15407/akademperiodyka.416.188
4. Panko AV, Kovzun IG, Ulberg ZR, Oleinik VA, Nikipelova EM, Babov KD (2016) Colloid-chemical modification of peloids with nano- and microparticles of natural minerals and their practical use. In: Fesenko O, Yatsenko L (eds) Nanophysics, nanophotonics, surface studies, and applications. vol 183 Springer PROCEEDINGS IN PHysics, Cham, pp 163–177. https://doi.org/10.1007/978-3-319-30737-4_14
5. Panko AV, Kovzun IG, Nikipelova OM et al (2019) Nanostructural effects in iron oxide silicate materials of the Earth’s crust. In: Fesenko O, Yatsenko L (eds) Nanophysics, nanophotonics, surface studies and applications. Springer proceedings in physics, vol 221. Springer, Cham, pp 367–386. https://doi.org/10.1007/978-3-030-17759-1_25
6. Panko AV, Kovzun IG, Nikipelova OM et al (2018) Nanostructural and nanochemical processes in peloid sediments aided with biogeocenosis. In: Fesenko O, Yatsenko L (eds) Nanophysics, nanophotonics, surface studies and applications. NANO 2017. Springer proceedings in physics, vol 214. Springer, Cham, pp 215–230. https://doi.org/10.1007/978-3-319-92567-7_13
7. Tarasevich YuI, Ovcharenko FD (1975) Adsorbtsiya na glinistyih mineralah (Adsorption on clay minerals) (in Russian). Naukova dumka, Kyiv
8. Kovzun IG, Ulberg ZR, Panko AV, Prokopenko VA, Oleinik VA, Nikipelova EM (2015) Colloid-chemical and nanochemical processes in peloids on basis of ferrous clay minerals. In: Fesenko O, Yatsenko L (eds) Nanoplasmonics, nano-optics, nanocomposites, and surface studies. Springer proceedings in physics, vol 167. Springer, Cham, pp 233–243. https://doi.org/10.1007/978-3-319-18543-9_15
9. Panko AV, Kovzun IG, Prokopenko VA, Tsyganovich OA, Oliinyk VO, Nikipelova OM (2017) Nano- and microdisperse structures in processes of metamorphism, reduction sintering, and component separation of iron-oxide-silicate materials. In: Fesenko O, Yatsenko L

(eds) Nanophysics, nanomaterials, interface studies, and applications. NANO 2016. Springer proceedings in physics, vol 195. Springer, Cham, pp 743–755. https://doi.org/10.1007/978-3-319-56422-7_57

10. Ulberg ZR, Pertsov NV, Garbara SV, Nechaev SV, Stepanenko VG (1990) Silikatnyie bakterii v protsessah mikrobiologicheskogo vyischelachivaniya metallov iz rud (Silicate bacteria in the processes of microbiological leaching of metals from ores). Doklady AN USSR, Series B 5:80–83
11. Brierly IA (2007) Biohidrometallyrgy—this microbiologist's perspective. Adv Mater Res 20–21:3–10. https://doi.org/10.4028/www.scientific.net/amr.20-21.3
12. Rozanov AY, Zavarzin GA (1997) Bacterial paleontology. Her Russ Acad Sci 67(6):241–245
13. Panko AV, Kovzun IG, Prokopenko VA, Nikipelova OM, Tsyganovich OA, Oliinyk VO (2021) Catastrophic phenomena on marine slopes and in artificial dams in a presence of nanostructured iron-aluminosilicates. In: Fesenko O, Yatsenko L (eds) Nanomaterials and nanocomposites, nanostructure surfaces, and their applications. Springer proceedings in physics, vol 246. Springer, Cham, pp 381–395. https://doi.org/10.1007/978-3-030-51905-6_28
14. Verhoogen I, Turner FI, Weiss LE, Wahrhaftig C, Fyfe WS (1970) The Earth. An introduction to physical geology. Holt. Rinehart and Winston Inc, New York-Montreal-London-Sydney
15. Sherbak NP, Pavlishin VI, Litvin AL et al (1990) Mineralyi Ukrainyi: Kratkiy spravochnik (Minerals of Ukraine: A Quick Reference). Naukova dumka, Kyiv
16. Weyl PK (1970) An introduction to the marine environment. John Wiley and Sons, New York
17. Kessler YuM, Zaitsev AL (1989) Solvofobnyie effekty (Solvophobic effects). Himiya, Leningrad
18. Yahnin ED (1995) Leading scientists in colloid science of CIS (Vedushie uchenye-kolloidniki stran SNG). Russian Academy of Sciences, Moscow (in Russian)
19. Burkinskii BV, Babov KD, Nikipelova OM et al (2019) Kuyalnytsky estuary: realities and prospects of recreational use (Kuyal′nyts′kyy lyman: realiyi ta perspektyvy rekreatsiynoho vykorystannya) (in Ukrainian). Helgenetika, Odessa
20. Nasibullin BA, Gushcha SG, Nikipelova OM, Nikolenko SI et al (2007) Patofiziolohichni mekhanizmy biolohichnoi aktyvnosti kolorovykh hlyn (Pathophysiological mechanisms of biological activity of colored clays). Kharkiv. ISBN 978-966-400-418-0
21. Gomes CSF, Rautureau M, Gomes JHC, Silva EAF (2021) Interactions of clay and clay minerals with the human health. In: Gomes C, Rautureau M (eds) Minerals latu sensu and human health. Springer, Cham. https://doi.org/10.1007/978-3-030-65706-2_7
22. Gomes CF, Gomes JH, da Silva EF (2020) Bacteriostatic and bactericidal clays: an overview. Environ Geochem Health 42:3507–3527. https://doi.org/10.1007/s10653-020-00628-w
23. Emel'janov VA (2003) Osnovy morskoj geoekologii (Basics of marine geoekology). Kyiv, Naukova dumka
24. Panko AV, Kovzun IG, Nikipelova OM, Prokopenko VA, Tsyganovich OA, Oliinyk, VO, Kosorukov PO (2020) Chemical and geochemical transformations of pelitic (therapeutic) materials under the influence of biocolloid processes. Chem Phys Technol Surface: Proc. Ukr. Conf. Intern. Participation. 21−22 October 2020. Kyiv: ISC: P 136
25. Voitenko YI (2019) Synergetics of geological mediums and its impact on the effectiveness of the exploitation and exploration for mineral deposits. Mineral Res Ukr 3:15–21. https://doi.org/10.31996/mru.2019.3.15-21